Revisit to the RXTE and ASCA data for GRO J1655-40: Effects of Radiative Transfer in Corona and Color Hardening in the Disk

S.N. Zhang[1,2], Xiaoling Zhang[1], Xuebing Wu [3], Yangsen Yao[1], Xuejun Sun[1], Haiguang Xu[4], Wei Cui[5], Wan Chen[6,7], B.A. Harmon[2], C.R. Robinson[8]

ABSTRACT

The results of spectral modeling of the data for a series of RXTE observations and four ASCA observations of GRO J1655-40 are presented. The thermal Comptonization model is used instead of the power-law model for the hard component of the two-component continuum spectra. The previously reported dramatic variations of the apparent inner disk radius of GRO J1655-40 during its outburst may be due to the inverse Compton scattering in the hot corona. A procedure is developed for making the radiative transfer correction to the fitting parameters from RXTE data and a more stable inner disk radius is obtained.

A practical process of determining the color correction (hardening) factor from observational data is proposed and applied to the four ASCA observations of GRO J1655-40. We found that the color correction factor may vary significantly between different observations and the finally corrected physical inner disk radius remains reasonably stable over a large range of luminosity and spectral states.

Subject headings: accretion, accretion disks — black hole physics — stars: individual (GRO J1655-40) — X-rays: stars

1. Introduction

The X-Ray Nova GRO J1655-40 (Nova Scorpii 1994) was discovered by the Burst and Transient Source Experiment (BATSE) onboard the *Compton Gamma Ray Observatory* on July

[1]Physics Department, University of Alabama in Huntsville, Huntsville, AL 35899; zhangsn@email.uah.edu, xizhang@jet.uah.edu

[2]Space Sciences Lab., SD50, NASA Marshall Space Flight Center, Huntsville, AL 35812

[3]Beijing Astronomical Observatory, Chinese Academy of Sciences, Beijing 100012, China. P.R.

[4]Physics Department, Shanghai Jiaotong University, Shanghai, 210000, P.R. China

[5]Center for Space Research, MIT, Cambridge, MA 02139; cui@space.mit.edu

[6]Dept. of Astronomy, University of Maryland, College Park, MD 20742

[7]NASA/Goddard Space Flight Center, Code 661, Greenbelt, MD 20771

[8]NSF

27, 1994 (Zhang *et al.*, 1994). Superluminal jets were soon observed at radio frequencies from the system (Tingay *et al.*, 1995; Hjellming and Rupen, 1995) in close correlation with its hard X-ray activities (Harmon *et al.*, 1995), thus suggesting its similar nature to the black hole candidate and the first microquasar GRS 1915+105 (Mirabel and Rodriguze, 1998). Optical observations allowed precise determination of the parameters of the binary system: mass of the compact object of $7.02 \pm 0.22\ M_{\odot}$, inclination of $i = 69.50 \pm 0.08°$ degrees and a mass ratio of $Q = 2.99 \pm 0.08$ (Orosz & Bailyn 1997). Similar, yet more conservative estimate of the black hole mass obtained by Shahbaz *et al.*(1999) is $6.0 \pm 0.2\ M_{\odot}$. These results thus provide so far the best evidence for the black hole nature of the compact object in GRO J1655-40.

The proximity of GRO J1655-40 and its well determined system parameters make it one of the best laboratories for studying several important astrophysical subjects: accretion disk physics, jet/outflow production and transportation, general relativity in the strong field limits, etc. Some of these results have already been reported. Hameury *et al.*(1997) suggested that the first observed optical brightening prior to an X-ray outburst in GRO J1655-40 (Orosz *et al.*, 1997b) provides evidence for the advection dominated accretion flow (ADAF) in the quiescent state of black hole X-ray binaries (Narayan and Yi, 1995; Narayan, 1995). Zhang, Cui and Chen (1997b) made the first determination of the black hole angular momentum of GRO J1655-40, making use of the high quality energy spectrum of the source observed with ASCA (Zhang *et al.*, 1997a). The estimated near maximal black hole spin rate in GRO J1655-40 and the other microquasar GRS 1915+105 suggests that the highly relativistic jets may be related to the angular momentum of the black holes (Blandford and Znajek, 1977). Cui, Zhang and Chen (1998) have also proposed that the ~300 Hz QPO observed in GRO J1655-40 (the highest frequency from any black hole system) is the frame dragging effects around a rapidly spinning black hole, predicted in Einstein's general relativity. If confirmed, this would be one of the first cases of observational verification of general relativity effects near the strong field limit. More recently, Zhang *et al.*(2000) discovered the three-layered accretion disk structure in the two microquasars GRO J1655-40 and GRS1915+105, making use of the ASCA and RXTE data. The similarity between the accretion disk structure and the solar atmosphere suggests that magnetic fields may play very important roles in the accretion process, high energy electron acceleration, high energy radiation and outflow/jet production.

However, one fundamental and unsolved question in the accretion disk physics is whether the inner disk boundary is stable, especially in the high luminosity state of black hole X-ray binaries. In the quiescent state the inner portion of the geometrically thin and optically thick disk is most likely truncated very far away from the black hole horizon, and replaced by a hot, optically thin and nearly spherical accretion flow. This is the well known ADAF solution. Alternative outflow may dominate inward accretion and the near-Keplerian disk may still extend very close to the black hole horizon (Blandford and Begelman 1999). Observationally the two scenarios are still indistinguishable, due to the limitations of the currently available X-ray instruments. In the high accretion state the disk is generally believed to be able to extend very close to the black hole horizon, because strong X-ray emissions are observed, indicating that the conversion efficiency

from the gravitational potential energy into radiation energy is high, and thus the inner disk radius should not be very large. It is however not clear if the inner disk boundary may stay stably at the last stable orbit of the black hole, regardless of the luminosity and spectral states of the source. This issue is very important since if the inner disk radius varies significantly, one must be very careful in determining the radius of the last stable orbit, and thus the previously reported determination of black hole angular momentum may be questionable.

Significant inner disk radius variations have been reported in GRS 1915+105 (Belloni *et al.*, 1997) and the variations are found to be consistent to the thermal and viscous time scales of the disk at various radii. However, recently Merloni *et al.*(1999) suggested that these variations might be due to the variations of the disk structure, which resulted in the variations of the color hardening factor, and thus made the apparent and uncorrected inner disk radius highly variable. In GRO J1655-40 and several other black hole X-ray binaries, the apparent inner disk radii inferred from X-ray spectral modeling have also been found to vary significantly. Here in this paper we report our re-analysis of some of these data, with the incorporation of a radiative transfer correction procedure, because some of the photons emitted from the accretion disk could not reach the observer directly; they are converted to hard X-ray photons by the hot electrons in the corona around the black hole. The details of the radiative transfer correction are presented in Appendix A. We also propose a procedure for the determination of the color hardening factor from data; the procedure is presented in Appendix B. Our results demonstrate that the inner disk radius in GRO J1655-40 is consistent with being a constant; the apparent and uncorrected inner disk radius variations are due to both the radiative transfer and color hardening processes in the inner disk region. The angular momentum of the black hole in GRO J1655-40 is found to be near maximal, consistent with early reports by some of us (Zhang *et al.*, 1997; Zhang, Cui and Chen 1997; Cui, Zhang and Chen 1997).

2. Data Selection and Analysis

2.1. Data Selection

Like typical BHC (black hole candidate) in X-ray binary system, GRO J1655-40 underwent a rising phase, a very-high/hard state, a high/soft state and a low/hard state in the 1997 outburst (Sobczak *et al.*, 1999), as shown in Fig. 1. Some typical spectra in these states are shown in Fig. 2. We present 38 observations, as shown in Fig. 1 , covering primarily the very-high state (in which the source underwent a complex spectra variation) of the 1997 outburst of GRO J1655-40 obtained with PCA (Proportional Counting Array) onboard RXTE; Sobczak *et al.*(1999) reported significant inner disk radius variation during this period. The "standard2" mode data are used, which correspond to 129 channels from 0–100 keV. The PCA is made of five PCUs. Considering instrument response, only data from PCU0 and PCU1 in the energy range 2.5 – 20 keV are used (Sobczak *et al.*, 1999). The response matrix is Keith Jahoda's 1998 January version. The

background spectra are obtained using the standard background model for bright sources. The spectra are extracted separately for each PCU and fitted simultaneously using XSPEC. A 1% systematic error was included in the fitting.

Four observations of the bright state of GRO J1655-40 have been made with ASCA since its launch. Its excellent response in low energy range provides us with the possibility of studying the spectrum in this area. The GIS2 events were collected within a circular region with radii between 5' and 6' centered at the source positions. Background was not substracted. The GIS2 data in the energy range of 0.7 – 10 keV are used in our analysis. For one of these observations we also have a simultaneous RXTE observation, which allows us to evaluate and compare the relative normalization of the RXTE/PCA and the ASCA/GIS instruments. This observation of ASCA lasted for two days. When doing the ASCA-XTE joint fitting, we only used the data collected simultaneously with RXTE.

2.2. Fitting Models and Parameters

Traditionally the continuum spectra of black hole X-ray binaries have been fitted with a two-component model, a soft component approximated by a disk-blackbody-like spectrum, and a hard component approximated by a power-law-like model with a high energy cutoff. For reasons discussed in Appendix A, we replace the power-law component with the thermal Comptonization model of Titarchuk (*compTT* in the XSPEC package, Titarchuk *et al.*, 1995). In this model, the seed photons to the Comptonization process are assumed to have a characteristic energy, which corresponds roughly to the lower end cutoff of the Comptonized component. The higher end cutoff corresponds to the characteristic energy of the hot electrons. The comparison of the two models is shown in Fig. 3.

Thus the general model we employed for the continuum spectra is: $wabs(diskbb + compTT)$. For the observations only with the RXTE instrument, the neutral hydrogen column density is fixed at 0.66, which is inferred from the ASCA and RXTE joint fitting of the simultaneous RXTE and ASCA observations, which occurred in the high/soft state of GRO J1655-40, in which the hard component can be ignored below 10 keV. In the rising phase and the high/soft state, an absorption edge is required for the fitting. Sometimes a line feature is also required. Because our main objective is to quantify the continuum spectra, the edge and line parameters are not presented in this paper.

In the RXTE/ASCA joint fitting, for the two data sets we use the same model and parameters, except for the different scaling factors, i.e., the model becomes $wabs(diskbb + compTT)constant$, in which *constant* is fixed to unity for the RXTE data and allowed to float for the ASCA data. For three of the four ASCA observations, the soft component can also be fitted with the *compTT* model. The parameters of the two models for the same data will give us some understanding of the hardening process in the disk.

The fitting parameters for the RXTE observations are listed in Table 5 and shown in Fig. 4. It can be seen that in the very-high/variable state, the soft component normalization varies dramatically, and there is a significant anti-correlation between the hard photon flux and the soft component normalization. The fitting parameters for the ASCA observations are listed in Table 5 and shown in Fig. 6. The ASCA–RXTE joint fitting results are shown in Table 2 and shown in Fig. 5.

3. Results

3.1. Interpretation of the multi-color disk black-body

The inner radius of the disk around the black hole may be estimated if the parameters of the *diskbb* component are determined from the X-ray spectral fitting. In the soft state in which the hard component is negligible, we might consider that no photons emitted from the disk are scattered to the hard component, i.e., all disk photons escape from the system and reach the observer (albeit to the interstellar absorption and the limited detector area and response, which may be corrected after the observations). Thus the multicolor disk normalization parameter is related to the inner disk radius in the following equation (Makishima *et al.*, 1986):

$$K = \left(\frac{R_{\rm in}}{\rm km}\right)^2 \left(\frac{D}{10\ \rm kpc}\right)^{-2} \cos\theta, \tag{1}$$

where $R_{\rm in}$ is the inner disk radius in kilometers, D is the distance to the source in kpc, θ is the inclination angle of the disk. The geometric parameters of GRO J1655-40 are well-determined from optical observations: $\theta = 69.5^\circ \pm 0.1^\circ$ (Orosz & Bailyn, 1997), $D = 3.2 \pm 0.2$ kpc (Hjellming & Rupen, 1995). The inner disk radius can thus be determined from this relation.

If the hard component is comparable or stronger than the soft component, the observed soft component cannot be considered as the original disk emission spectrum. This is because some of the disk photons are Compton scattered to form the hard component, and consequently the observed soft component is only a portion of the original disk spectrum. Therefore the normalization parameter inferred from the direct spectral fitting under-estimates the original disk emission significantly. Assuming that the disk photons are the main source of the seed photons of the Comptonization process responsible for the hard X-ray component, it is possible to make a radiative transfer correction in order to restore the original disk emission spectrum. The commonly observed hard and soft flux anti-correction provides a strong support to the assumption that the disk photons are the main source of seed photons. We have thus developed a procedure for the radiative transfer correction, as presented in Appendix A. Reliable hard component parameters are required for the radiative transfer correction, which can be obtained from the RXTE data. The ASCA data are usually not sufficient for determining the hard component reliably, because the ASCA instruments lack any useful response above 10 keV.

However, an appropriate color correction should be also applied to get the physical inner disk radius, due to the saturated electron scattering of the original blackbody photons in the inner disk region, where electron scattering dominates the free-free absorption completely. Assuming that the electron scattering changes the temperature $T_{\rm eff}$ of the soft component by a factor of f, i.e., the temperature becomes $fT_{\rm eff}$, the actual inner disk radius should be $R_{\rm eff} = f^2 R_{\rm in}$. The commonly used color correction factor from Shimura & Takahara (1995) is $f = 1.7 \pm 0.2$. However, the color factor might not be constant; it should change with the disk structure. Recently Merloni *et al.*(1999) suggested that the color correction factor might range from 1.5 to 3, thus indicating the estimated inner disk radius may be quite uncertain, unless the color hardening factor is known reliably. In Appendix B, we propose for a procedure to determine the color correction factor reliably from the same spectral data, provided that the instrument has sufficient low energy response and resolution, such as the ASCA instruments, but not the RXTE instruments.

Thus the appropriate procedure for estimating the physical inner disk radius after the two-component spectral fitting should be: 1) do Comptonization correction if the hard component is not negligible, and 2) do color correction, if the color correction factor may be determined from the data reliably.

3.2. Radiative Transfer Correction

Fig. 4 and Table 5 shows the spectral fitting results for the 38 RXTE/PCA observations, as well as the corrected normalization parameter of the disk-blackbody component after the radiative transfer correction procedure is applied. It is clear that before the correction, the normalization parameter varies significantly and is anti-correlated with the hard X-ray photon flux. After the radiation transfer correction, the new normalization parameter, which is proportional to R^2, does not vary very much, and thus implies that the inner accretion disk radius is probably stable. However, the inner disk radius cannot be estimated reliably from the PCA/RXTE data alone, because the precise value of the color correction factor cannot be obtained.

3.3. Color Correction

Though it is difficult to obtain hard component parameters reliably with the ASCA data, fortunately in all four ASCA observations the hard component is very weak, as determined from the simultaneous CGRO/BATSE and RXTE observations. Therefore the Compton radiative transfer correction is not important; only one of them needs minor radiative transfer correction. Fig. 6 shows the energy spectra from several ASCA observations. Table 5 shows the fitting parameters of the ASCA data, the value of color correction factor, the normalization parameters from these observations (see Appendix B for details). The data from the first observation cannot be fitted with the *diskbb* model, because the optical depth is small, and the energy difference

between the incident photons (T_0) and the hot electrons (kT) is large. This suggests that the spectrum shape cannot be well described by a thermal spectral model, and the color correction factor is not meaningful in this case. It can be seen that the color correction factor is not a constant; the range of the color correction variation is consistent to the prediction of Merloni et al (1999). Because the exact value of the interstellar absorption is unknown, the estimated parameters suffer significant uncertainties, as shown in the table.

Assuming that the inner disk radius is the last stable orbit of the black hole and following the procedure in Zhang, Cui and Chen (1996 **Which is this?**), we estimate that the black hole angular momentum of GRO 1655-40 is around between 0.8–1.0 GM/c^2, consistent to an extremal Kerr black hole.

3.4. Relative Calibration Issue of ASCA and RXTE

We want to address briefly the relative calibration issue between RXTE/PCA and ASCA/GIS. Fig. 2 and Table 2 show the model-fitting results for the simultaneous RXTE and ASCA observations on July 26, 1997. Clearly there is a significant difference between the calibration of ASCA/GIS and RXTE/PCA for the soft component. For this observation the RXTE/PCA overestimated the low energy flux significantly, if we trust the absolute calibration of the low energy response (around 1 keV) of ASCA. One therefore must be very careful in interpreting the model fitting results using any RXTE/PCA low energy data (roughly below 5 keV).

4. Discussion

The application of the thermal Comptonization spectral model *compTT* to the hard component and the subsequent radiative transfer correction procedure are only valid to a certain extend. If the source of the seed photons is not the soft component, the whole radiative transfer correction procedure is not meaningful at all. However, as shown in detail by Zhang *et al.*(2000), the characteristic photon energy of the seed photons is very close to that of the disk photons, as determined with the ASCA data. This thus suggests that the dominant source of the seed photons is indeed the soft component, at least during these ASCA observations. However, if there is evidence for other significant source of seed photons, we must take this into account in the radiative transfer correction process.

It has been shown from some high energy observations extending beyond several hundred keV that the high energy electrons responsible for the Comptonization process in the corona may have a non-thermal energy distribution. In this case the parameters derived for the *compTT* model are not meaningful physically. However, because the radiative transfer correction procedure only uses the total photons in the hard component, the final normalization parameter derived after the

correction process should still be valid.

The fundamental limitations of the radiative transfer correction procedure are related to the assumptions made for the properties of the corona, which is assumed to have a spherical shape with a density profile of $1/R$ and a truncation outer radius constant during all observations. We have not studied quantitatively the uncertainties introduced by any deviations of the assumptions from the real corona. However, our results imply that the correction procedure probably has taken the main physical effects into account, because the corrected inner disk radius appears to be quite stable for most of the observations. One way for calibrating our model is to compare the corrected inner disk radius with that inferred from the soft state, in which no radiative transfer correction is needed. It can be seen from our data that by choosing an appropriate outer truncation radius of the corona, the corrected inner disk radius from all observations in the very-high/variable state may be quite consistent with that inferred in the soft state (the inner disk radius in the soft state has always been found to be very stable).

The procedure for determining the color correction factor is also subjected to a number of uncertainties. The first source of possible uncertainties is the assumptions in the *compTT* model (when used for the soft component): the electrons have a Maxwellian energy distribution, the scattering geometry is either spherical or disk-like, and the seed photons have a characteristic energy and are all originated from the center of the scattering medium. These assumptions, however, may not differ from the actual accretion disk structure significantly. First, because the inner region should be radiation pressure dominated, the disk temperature varies very slowly with radius ($T(r) \propto r^{-3/8}$), as opposed to a more rapid temperature variation in the gas pressure dominated disk ($T(r) \propto r^{-3/4}$) (Liang 1999). Second, nearly all gravitational energy is released in a very small region around the inner disk boundary, thus the point and central source assumption is also not violated significantly.

The second source of possible uncertainties is in the assumption that the soft component may be modeled as a disk-blackbody spectrum, in order for deriving the inner disk radius. Clearly the whole soft component cannot be described with the disk-blackbody model, due to the saturated Compton scattering in the disk region. However, since the main purpose of the model fitting is determining the flux in the soft component, and the disk-blackbody model does provide adequate fit to the high energy end of the *compTT* spectrum (as shown in Fig. 10), we believe it is a good approximation to use the *diskbb* model for the soft component. Therefore we conclude that color correction procedure we proposed is a reasonably reliable approach for determining the actual color correction factor from observation data. In fact the estimated color correction factors agree quite well with the possible values calculated from numerical analysis of the accretion disk structure (Merloni *et al.*, 1999).

The detailed physical processes occurring in the disk and corona are not addressed in this paper. We refer readers to another publication by some of us, in which we have identified a three-layered structure of the accretion disk, very similar to the solar atmosphere; between the

commonly known cold disk and the hot corona, there also exists a warm layer, which is actually responsible for regulating the observed soft component, i.e., the color hardening process (Zhang *et al.*, 2000).

5. Conclusions

We have re-analyzed some of the RXTE/PCA data of the microquasar GRO J1655-40 and confirmed qualitatively the previously reported significant variations of the apparent inner accretion disk radius, before the color and radiative transfer corrections. However, our final results are quite different from the earlier ones, because we applied a physical model for the hard component (*compTT*), instead of the commonly employed phenomenological power-law model. The inner disk radius inferred directly from the spectral fitting varies dramatically between observations, if no Comptonization radiative transfer and color corrections are applied. After the Comptonization correction and color correction, the inner disk radius becomes quite stable. We therefore conclude that the inner disk radius in the microquasar GRO J1655-40 remains remarkably stable in a span of several years whenever the source is observed in a bright state; the corrected inner disk radius is apparently independent of the flux and spectral state of the source. (Note that our conclusion is irrelevant to the quiescent state of the source.)

The stability of the inner disk boundary in GRO J1655-40 further supports that the compact object in the center of the accretion disk is a black hole, because the radius of the inner disk is expected to vary with mass accretion rate if the compact object is instead a neutron star, due to the interaction between the disk and the neutron star magnetosphere and/or the radiation drag of the surface X-ray emission of the neutron star. Using the ASCA data we are also able to derive the color correction factor from the data; the color correction factor changes significantly for different state of the source. Applying color corrections to the *diskbb* component derived with the ASCA data, we infer that the angular momentum of the black hole in GRO J1655-40 is around 0.8–1.0 GM/c^2, consistent with some previous reports (Zhang *et al.*, 1996, Zhang, Cui & Chen 1996; Cui, Zhang & Chen 1997; **Kaaret ?**).

The success of the simple Comptonization radiative transfer correction thus provides strong support to the Comptonization origin of the hard photons and indicates that the dominant source of seed photons to the Comptonization process in the corona is the soft photons from the disk. It is interesting to note that the outer truncation radius of the corona is quite large (800 r_g), in order for the inner accretion disk radius in the very-high/variable state to be consistent with that determined in the soft state.

RXTE/PCA alone cannot be used to determine the color factor, due to the poor response of PCA below 2.5 keV. The inconsistency between the normalization parameter for the soft component between the RXTE/PCA and the ASCA/GIS instruments suggests that the absolute value of the *diskbb* normalization parameter (therefore the inner disk radius) cannot be determined

with the RXTE/PCA data alone, again due to the poor low energy response of the RXTE/PCA instrument.

This work was supported, in part, by NASA grant NAG5-7665.

Appendix A. Radiative Transfer Correction to the Soft Component

Neglecting some line and edge features in the X-ray spectrum of a black hole X-ray binary, the conventionally used two-component spectral model, i.e., multi-color disk blackbody component plus a power-law component with a high energy cutoff, is over-simplified in two aspects:

First, the assumption that the power-law component extending straight to the low-energy limit of the spectrum is non-physical, since the power-law component is believed to be produced by inverse Compton scattering of low-energy photons by high energy electrons. The most natural source of the seed photons is the blackbody-like component produced from the accretion disk. Therefore a sharp low-energy cutoff or turn-over must be present in the power-law component in the low-energy region, since the blackbody-like soft component has a peak temperature, i.e., a turn-over in the low-energy end. Usually the observed peak temperature is between 2 to 5 keV, thus requiring a sharp cut-off or turn-over of the power-law component roughly below 2 to 5 keV. Neglecting this low-energy cutoff by applying a simple power-law spectrum model would under-estimate the flux in the soft blackbody-like component; the amount of under-estimation is apparently correlated with the shape and flux of the power-law component.

Secondly, it has been a rather standard approach by many (including the authors of this paper) in the field to take the blackbody-like flux derived from the spectral model fitting as the true flux of the accretion disk. This ignores the radiative transfer process in the production of the power-law component. Since the power-law component is likely produced by scattering the soft photons in the original blackbody-like component of the accretion disk, each photon in the power-law component comes at the expense of a lost photon in the blackbody-like component, even if no absorption occurs in the Comptonization process. Therefore one must correct for this radiative process in order to infer the original flux of the blackbody-like component. Since the power-law production region cannot cover the entire accretion disk uniformly, the amount of correction to the blackbody-like component is thus energy dependent. Therefore ignoring this correction would result in under-estimation of the flux of the blackbody-like component.

The above two problems tend to under-estimate the flux in the blackbody-like component, and are related to the co-existence of the hard X-ray power-law component. We thus expect that in the absence of any significant hard X-ray component (the conventionally called soft or high state), none of the above problems will cause any significant under-estimation of the blackbody-like flux. Indeed for all sources we know so far the inferred inner accretion disk radius is remarkably constant when no significant hard X-ray flux is observed (Sobczak *et al.*, 1999a; 1999b). Therefore the inner accretion disk radius inferred when a system is in a high or soft state may indeed be the last stable orbit of the blackhole, although cares must be taken when the absolute value of the inner disk radius is estimated, since the absolute flux calibration of the instruments used must be known very well, as well as several correction factors must be applied (Zhang, Cui and Chen 1997), even after the true luminosity of the accretion disk is derived from the observation.

Ideally one would like to have a full physical model, in which the blackbody-like component

Table 1. Fitting and corrected results using RXTE/PCA data

Date	MJD	T_{in}	K_{bb}		Photon flux[a]		Energy flux[b]		count-rate[c]	χ^2_ν/dof	n_e[d]
		(keV)	fitting	corrected[e]	soft	hard	soft	hard	(pcu0)		
960509	50212.6	$1.39^{+0.06}_{-0.03}$	434^{+111}_{-134}	881	2.68	3.54	1.77	2.23	3378.0	1.43/83	14.9
960510	50213.4	$1.46^{+0.07}_{-0.04}$	322^{+89}_{-92}	781	2.46	4.02	1.66	2.50	3513.0	1.38/83	18.7
960511	50214.5	$1.46^{+0.07}_{-0.05}$	301^{+86}_{-91}	759	2.33	3.98	1.57	2.48	3415.0	1.61/83	19.5
960512	50215.3	$1.43^{+0.07}_{-0.04}$	364^{+99}_{-117}	800	2.56	3.76	1.71	2.38	3459.0	1.22/83	16.6
960514	50217.1	$1.43^{+0.06}_{-0.11}$	237^{+218}_{-70}	580	1.55	3.67	1.06	2.32	2856.0	1.47/83	23.7
960520	50223.6	$1.56^{+0.10}_{-0.35}$	168^{+69}_{-48}	484	1.66	3.92	1.16	2.45	3039.0	1.79/83	26.0
960527	50230.7	$1.28^{+0.03}_{-0.05}$	1273^{+309}_{-198}	1449	5.39	1.45	3.45	1.12	3853.0	0.96/83	2.7
960608	50242.5	$1.35^{+0.03}_{-0.05}$	777^{+126}_{-103}	1149	4.22	2.73	2.76	1.93	3860.0	1.01/83	8.2
960620	50254.5	$1.25^{+0.03}_{-0.03}$	1114^{+191}_{-155}	1318	4.28	1.95	2.72	1.73	3797.0	0.78/84	3.6
960620	50254.6	$1.20^{+0.02}_{-0.02}$	1772^{+131}_{-195}	1997	5.45	2.08	3.41	1.95	4462.0	0.97/83	2.5
960620	50254.7	$1.31^{+0.02}_{-0.02}$	1117^{+84}_{-55}	1493	5.21	2.99	3.37	2.43	4851.0	0.94/86	6.1
960630	50264.5	$1.34^{+0.00}_{-0.00}$	1364^{+29}_{-13}	1823	7.16	1.69	4.67	1.42	5102.0	0.69/86	6.1
960725	50289.3	$1.30^{+0.00}_{-0.00}$	1372^{+24}_{-22}	1882	6.24	1.87	4.02	1.54	4619.0	0.78/86	6.6
960801	50296.3	$1.69^{+0.01}_{-0.02}$	238^{+17}_{-18}	1555	3.48	7.69	2.50	6.34	7102.0	1.07/86	40.3
960806	50301.7	$1.50^{+0.03}_{-0.02}$	522^{+25}_{-66}	1681	4.53	5.39	3.09	4.36	6082.0	0.67/86	24.8
960815	50310.6	$1.28^{+0.01}_{-0.00}$	1353^{+23}_{-24}	1856	5.69	1.68	3.64	1.40	4172.0	1.04/86	6.6
960822	50317.4	$1.29^{+0.01}_{-0.01}$	1139^{+27}_{-26}	2198	5.05	3.37	3.25	2.72	4871.0	0.56/86	13.8
960829	50324.4	$1.54^{+0.02}_{-0.03}$	436^{+70}_{-43}	1699	4.29	6.80	2.96	5.68	5833.0	0.68/83	29.0
960904	50330.2	$1.29^{+0.01}_{-0.01}$	1347^{+26}_{-25}	2030	5.87	2.28	3.77	1.86	4640.0	0.77/86	8.7
960909	50335.9	$1.31^{+0.01}_{-0.01}$	1211^{+24}_{-23}	1917	5.60	2.47	3.62	2.00	4632.0	0.74/86	9.7
960920	50346.2	$1.27^{+0.00}_{-0.00}$	1404^{+25}_{-24}	1753	5.73	1.31	3.66	1.12	3968.0	0.75/86	4.7
960926	50352.2	$1.26^{+0.00}_{-0.01}$	1613^{+63}_{-28}	1651	6.37	0.36	4.06	0.37	2931.0	1.09/83	0.5
961003	50359.6	$1.26^{+0.01}_{-0.01}$	1617^{+49}_{-51}	1609	6.13	0.64	3.92	0.60	3772.0	1.00/86	1.3
961015	50371.4	$1.32^{+0.00}_{-0.00}$	1378^{+23}_{-22}	1605	6.75	1.08	4.38	0.98	4491.0	0.81/86	3.3
961022	50378.1	$1.32^{+0.00}_{-0.00}$	1411^{+22}_{-21}	1733	6.82	1.39	4.42	1.20	4692.0	0.49/86	4.3
961027	50383.6	$1.37^{+0.01}_{-0.01}$	1014^{+25}_{-24}	2091	5.77	3.94	3.79	3.15	5696.0	0.59/86	15.2
961102	50389.2	$1.48^{+0.02}_{-0.02}$	262^{+23}_{-19}	1648	2.12	6.22	1.44	5.19	5254.0	0.71/86	39.4
970105	50453.3	$1.10^{+0.00}_{-0.00}$	1386^{+27}_{-26}	1472	2.81	0.31	1.70	0.31	1611.0	0.82/86	1.2
970112	50460.0	$1.06^{+0.00}_{-0.00}$	1639^{+27}_{-31}	1687	2.75	0.16	1.64	0.16	1438.0	1.18/86	0.6
970120	50469.0	$0.94^{+0.00}_{-0.00}$	1872^{+35}_{-30}	1876	1.74	0.01	1.00	0.02	777.6	1.55/86	0.04
970126	50474.8	$0.98^{+0.00}_{-0.00}$	1767^{+31}_{-32}	1795	2.06	0.07	1.20	0.07	993.2	1.25/86	0.3
970226	50505.8	$1.09^{+0.01}_{-0.01}$	1934^{+74}_{-77}	1997	3.83	0.35	2.31	0.26	2083.0	1.48/83	0.7
970324	50531.7	$1.09^{+0.02}_{-0.01}$	1977^{+103}_{-175}	2056	3.94	0.43	2.39	0.32	2228.0	1.08/81	0.8
970430	50568.6	$1.10^{+0.02}_{-0.04}$	1688^{+177}_{-274}	1965	3.38	1.37	2.05	0.92	2463.0	1.10/83	3.2
970605	50604.3	$1.18^{+0.01}_{-0.01}$	1733^{+65}_{-60}	1765	4.96	0.26	3.08	0.22	2731.0	0.88/83	0.4
970708	50637.5	$1.06^{+0.00}_{-0.01}$	1841^{+64}_{-45}	1867	3.20	0.15	1.92	0.15	1658.0	0.63/83	0.3
970803	50663.7	$0.79^{+0.01}_{-0.01}$	2324^{+276}_{-117}	2485	0.81	0.12	0.44	0.10	382.3	1.05/83	1.4
970829	50689.2	$0.47^{+0.12}_{-0.13}$	176^{+2854}_{-139}	321	0.002	0.004	0.01	0.04	3.6	0.83/86	12.7

[a] phtons/cm^2/s, 2.5 - 20 keV

[b] 10^{-8} ergs/cm^2/s, 2.5 - 20 keV

[c] 2.5 - 20 keV

[d] Electron number density in the inner disk radius.

[e] Radiative transfer corrested normalisation of *diskbb* component. Refer to Appendix A for detail. The outer radius of the corona is set to $800r_g$. The corresponding electon densities are listed in the last column of this table.

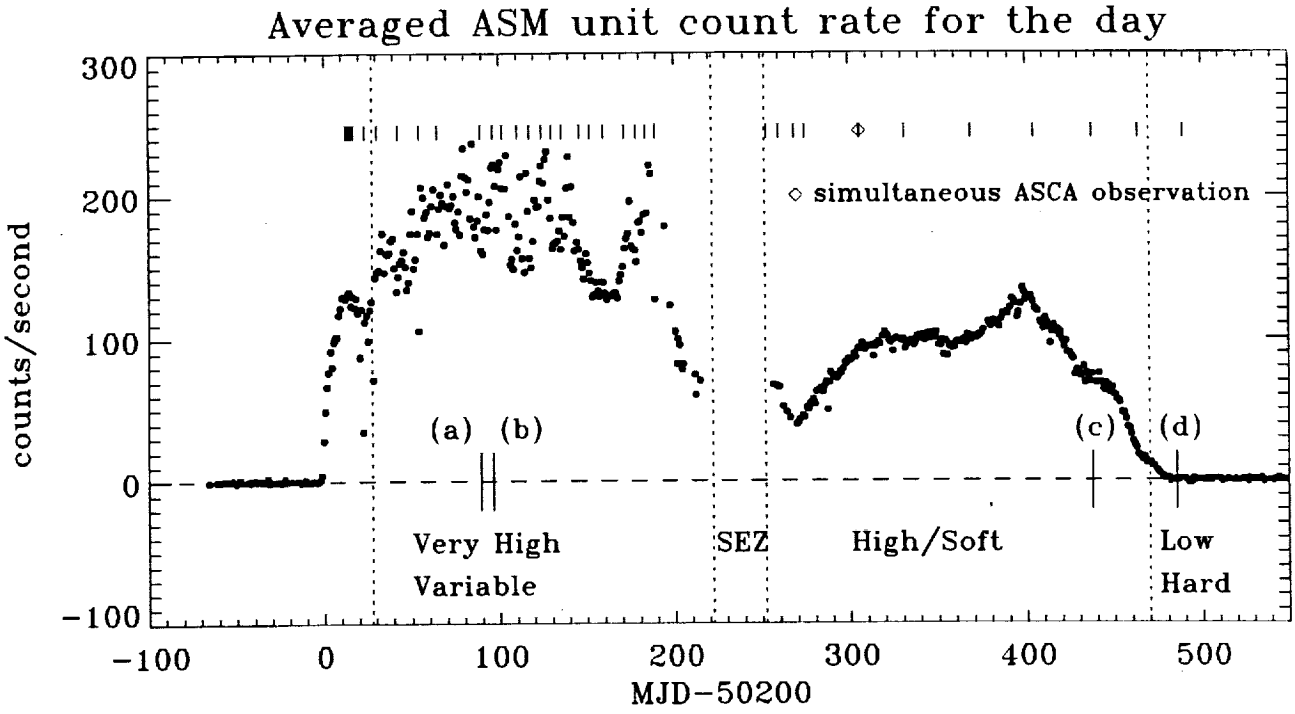

Fig. 1.— ASM light curve for the 1996-1997 outburst. The little vertical bars indicate the observations whose results are presented in this paper (Refer to Table 5). The dashed lines separate different states. Typical spectra for different state will be given for (a), (b), (c) and (d) (Refer to Fig. 2).

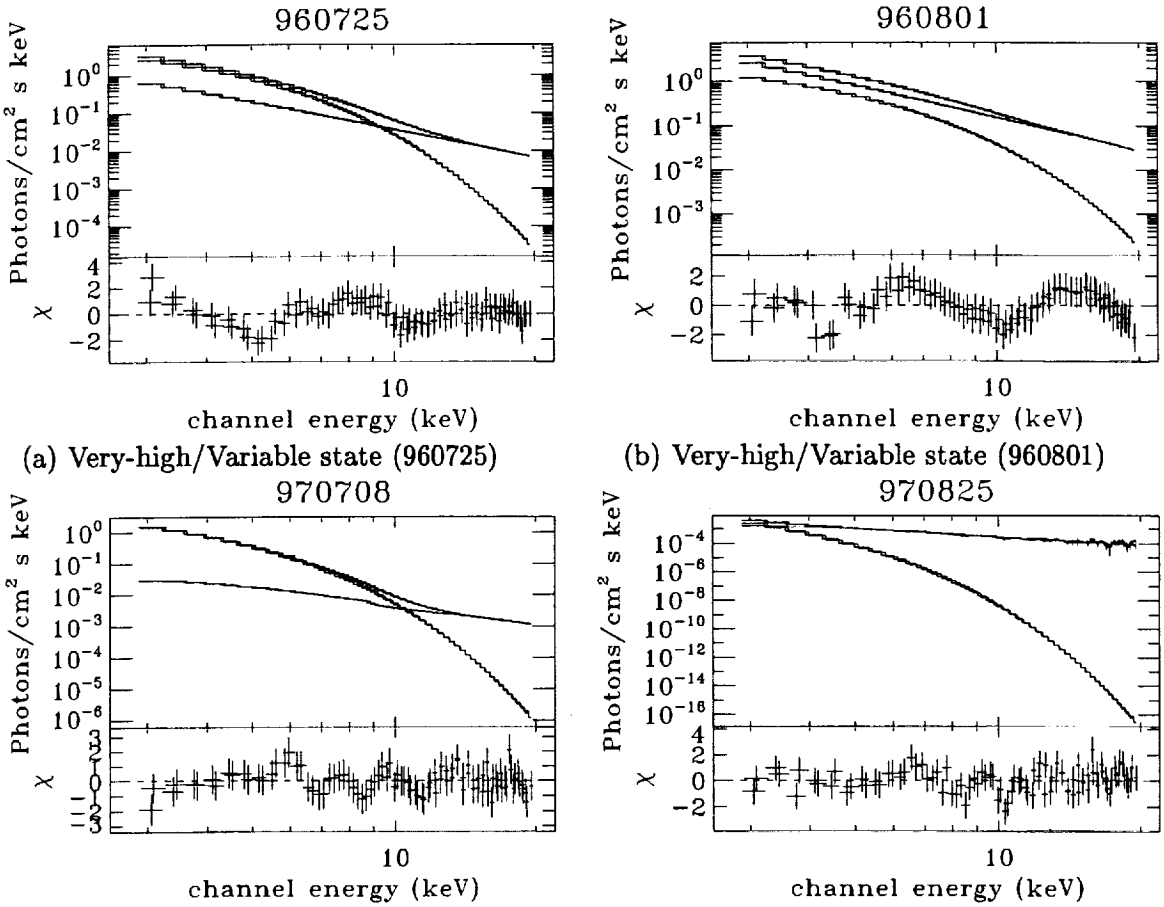

(a) Very-high/Variable state (960725)

(b) Very-high/Variable state (960801)

(c) High/Soft state (970708)

(d) Low/Hard state (970825)

Fig. 2.— Typical spectra in the three states. The upper panels are unfolded spectra, and the lower panels are residuals. The data from the four observations are fitted with the typical model we used: *wabs(diskbb+compTT)*. The upper two spectra, which are all in Very-high/Variable state, are only several days apart, but they are fundamentally different; in (a) the soft component dominates, while in (b) the hard component dominates. The effect of radiative correction is very significant in the cases in which the hard component dominates, while less significant or neglegible for soft states. (Refer to Table 5 and Fig. 4 for the effect of radiative correction.)

Table 2: Fitting parameters from ASCA and XTE observation of 970226. (See Fig. 5)

	nH (10^{22}cm^{-2})	$T_{\rm in}$ (keV)	*Norm*	T_0 (keV)	kT (keV)	τ
ASCA alone[a]	0.63	1.171	1196	-	-	-
XTE alone[b]	0.66 (fixed)	1.125	1817	1.5	49	1.6
Joint ASCA[b]	0.66	1.146	1310	0.14	66	1.6
Joint XTE[b]	0.66	1.146	1611	Same as above		

[a] Hard component is not significant under 10 keV.

[b] A smeared Fe absorption edge component is included, with the energy fixed at 8 keV, width fixed at 7 keV. (Sobczak *et al.*, (1999))

and the power-law component are coupled together self-consistently, i.e., some of the soft photons produced by the accretion disk are up-scattered by the high energy electrons into the power-law component; the amount of the soft photons to be scattered (also in a frequency-dependent way) and the shape and flux of the power-law component depend upon the geometry and energy distribution of the corona. However, such a model is not currently available in the field, and may not be practical to make, since many degrees of freedom necessarily exist for this model, in the absence of the detailed properties of the hard X-ray producing corona. Here we propose for a semi-physical model for addressing the existing problems of the simple two-component model.

Since the under-estimation of the flux of the blackbody-like component is most serious when the source is in a power-law bright state, whose power-law component usually exhibits a clear high energy cutoff above 100-300 keV, thermal Comptonization is the most likely mechanism for the power-law component production, although some non-thermal contribution, or a multi-temperature corona may be required in some cases. Because we are interested mainly in re-constructing the blackbody-like component reliably and the one-temperature thermal Comptonization model gives adequate description to the power-law component at low energies, we will only consider the one-temperature thermal Comptonization model for the power-law production in this paper.

Titarchuk and Lyubarskij (1995) have derived the analytical expression of the power-law component for the thermal Comptonization model in a self-consistent way, by assuming that the corona is in either a slab or spherical configuration with a uniform density and the soft photon source is located in the system of the corona. As will be discussed later, neither of these assumptions will likely introduce significant errors to the estimation of the blackbody-like component, as the final radiative transfer correction will at least partially compensate for the errors introduced by these assumptions.

We therefore replace the power-law component in the simple two-component model by the Titarchuk and Lyubarskij (1995) model (the *compTT* model in the *XSPEC* package). The

Table 3. ASCA fitting parameters, derived color correction factors and the black hole spin.

Date	diskbb			compTT				f[b]	$f^2\sqrt{K_{bb}}$	a[f]*
	nH[a]	T_{in} (keV)	K_{bb}	nH[a]	T_0 (keV)	kT (keV)	τ			
94/08/23[c]	...	...	...	0.26	$0.20^{+0.03}_{-0.02}$	1.56	8.1	...	...	...
Free nH										
94/09/27	0.27	$1.49^{+0.005}_{-0.004}$	192^{+2}_{-2}	0.39	$0.21^{+0.01}_{-0.01}$	1.21	12.3	$2.62^{+0.13}_{-0.13}$	95^{+9}_{-9}	$0.88^{+0.09}_{-0.09}$
95/08/15	0.69	$1.43^{+0.030}_{-0.020}$	[d]979^{+54}_{-58}	0.53	$0.39^{+0.01}_{-0.01}$	1.20	12.2	$1.36^{+0.04}_{-0.04}$	58^{+4}_{-4}	$0.98^{+0.07}_{-0.07}$
97/02/25	0.63	$1.17^{+0.004}_{-0.005}$	1196^{+22}_{-21}	0.54	$0.30^{+0.02}_{-0.02}$	0.99	13.4	$1.44^{+0.10}_{-0.10}$	72^{+10}_{-10}	$0.94^{+0.13}_{-0.13}$
Fix nH[e]										
94/09/27	0.27	$1.49^{+0.005}_{-0.004}$	192^{+2}_{-2}	0.27	$0.264^{+0.004}_{-0.004}$	1.19	13.0	$2.09^{+0.03}_{-0.03}$	60^{+2}_{-2}	$0.97^{+0.03}_{-0.03}$
95/08/15	0.69	$1.43^{+0.030}_{-0.020}$	[d]979^{+54}_{-58}	0.69	$0.282^{+0.005}_{-0.006}$	1.17	12.7	$1.88^{+0.06}_{-0.04}$	110^{+7}_{-6}	$0.80^{+0.05}_{-0.04}$
97/02/25	0.63	$1.17^{+0.004}_{-0.005}$	1196^{+22}_{-21}	0.63	$0.260^{+0.008}_{-0.008}$	0.99	13.2	$1.67^{+0.05}_{-0.05}$	96^{+6}_{-6}	$0.87^{+0.05}_{-0.05}$

[a]in unit of $10^{22}/\mathrm{cm}^2$

[b]Color correction factor, $f = T_{in}/T_0/2.7$

[c]Data from this observation cannot be fitted with *diskbb* model, so our method of deriving color correction factor cannot be applied to this data set.

[d]Radiative transfer corrected. The original value is 786.

[e]The nH is fixed to the value obtained from the fitting using *wabs(diskbb)* model.

[f]Estimated black hole spin in unit of GM/c^2.

high-energy cutoff of the power-law component is also taken into account self-consistently in this model. The spectral model is thus

$$F_x = wab(diskbb + compTT) \tag{2}$$

Assuming that all photons in the power-law component are produced by Comptonization of the photons in the disk blackbody-like component by high energy electrons in a corona above the disk, it is in principle possible to derive the original emissivity of the accretion disk by carrying out a radiative transfer correction. It is already known that a simple uniform corona model cannot be used to fit the observed data; a density distribution in the corona is required, although the detailed geometry is still not clear yet (Hua, Kanzanas and Cui 1998). Here we assume that the corona has a spherical geometry with radius R_0 and an electron density profile of:

$$n_e = n_{e,0}(r_g/R)^p \qquad (r_h < R < R_0) \tag{3}$$

where $r_g = \frac{GM}{c^2}$ is the gravitational radius of the black hole, r_h is the radius of the horizon of the black hole, p is index of the density profile and is taken to be unity for simplicity in this paper.

In practice R_0 may be determined approximately by examining the phase-lag spectrum of the light curve of a source. $n_{e,0}$ may in turn be determined by the optical depth inferred in the $compTT$ model, or by comparing the blackbody-like and the power-law fluxes derived in the spectral fitting, as will be illustrated later. This assumed corona geometry is not very different from that inferred by Hua, Kanzanas and Cui (1998) for Cyg X-1, except that we also take into account the black hole in the center in a very simple way.

We now consider a beam of photons emitted from a radius $r < R_0$ on the disk surface and along the direction with an angle θ from the disk surface. The optical depth for this beam can be described as:

$$\tau(r,\theta) = \int_0^{l_0} n_e a_e dl \tag{4}$$

where a_e is the Thomson cross section, $l_0 = -r\cos\theta + \sqrt{R_0^2 - r^2\sin^2\theta}$, which is the length of the path when the beam intersects the boundary of the sphere for $0 < \theta < \pi - \arcsin\frac{r_h}{r}$; if the beam reaches the black hole horizon before intersects the boundary of the corona, i.e., for $\pi - \arcsin\frac{r_h}{r} < \theta < \pi$, then $l_0 = -r\cos\theta - \sqrt{r_h^2 - r^2\sin^2\theta}$.

Substitute Eq. (3) and $R = \sqrt{r^2 + l^2 + 2rl\cos\theta}$ into Eq. (4), we obtain:

$$\begin{aligned} \tau_1(r,\theta) &= n_{e,0}a_e r_g \ln\frac{R_0 + \sqrt{R_0^2 - r^2\sin^2\theta}}{r(1+\cos\theta)} && (0 < \theta < \pi - \arcsin\tfrac{r_h}{r}) \\ \tau_2(r,\theta) &= n_{e,0}a_e r_g \ln\frac{r_h - \sqrt{r_h^2 - r^2\sin^2\theta}}{r(1+\cos\theta)} && (\pi - \arcsin\tfrac{r_h}{r} < \theta < \pi) \end{aligned} \tag{5}$$

The average probability $\bar{P}(r)$, which describes the probability that a disk photon is not scattered by an electron in the corona, can be calculated from $\tau_1(r,\theta)$ and $\tau_2(r,\theta)$:

$$\bar{P}(r) = \frac{\int_0^{\pi-\arcsin\frac{r_h}{r}} e^{-\tau_1(r,\theta)}\sin\theta d\theta + \int_{\pi-\arcsin\frac{r_h}{r}}^{\pi} e^{-\tau_2(r,\theta)}\sin\theta d\theta}{\int_0^{\pi}\sin\theta d\theta} \qquad (r_{in} < r < R_0) \tag{6}$$

where r_{rin} is the inner radius of the accretion disk.

If the photon is emitted from the disk surface outside the corona sphere, the average non-scattering probability $\bar{P}(r)$ can be expressed as:

$$\bar{P}(r) = \frac{\int_0^{\pi-\arcsin\frac{R_0}{r}} \sin\theta d\theta + \int_{\pi-\arcsin\frac{R_0}{r}}^{\pi-\arcsin\frac{r_h}{r}} e^{-\tau_3(r,\theta)}\sin(\theta)d\theta + \int_{\pi-\arcsin\frac{r_h}{r}}^{\pi} e^{-\tau_4(r,\theta)}\sin(\theta)d\theta}{\int_0^{\pi}\sin\theta d\theta} \qquad (r > R_0) \tag{7}$$

where $\tau_3(r,\theta)$ and $\tau_4(r,\theta)$ is described as

$$\begin{aligned} \tau_3(r,\theta) &= n_{e,0}a_e r_g \ln\frac{R_0+\sqrt{R_0^2-r^2\sin^2\theta}}{R_0-\sqrt{R_0^2-r^2\sin^2\theta}} && (\pi-\arcsin\tfrac{R_0}{r} < \theta < \pi-\arcsin\tfrac{r_h}{r}) \\ \tau_4(r,\theta) &= n_{e,0}a_e r_g \ln\frac{r_h-\sqrt{r_h^2-r^2\sin^2\theta}}{R_0-\sqrt{R_0^2-r^2\sin^2\theta}} && (\pi-\arcsin\tfrac{r_h}{r} < \theta < \pi) \end{aligned} \tag{8}$$

The equivalent optical depth $\tilde{\tau}(r)$ can then be calculated from

$$\tilde{\tau}(r) = -\ln\bar{P}(r) \tag{9}$$

where $\bar{P}(r)$ may be calculated from Eqs. (6) and (7) for $r < R_0$ and $r > R_0$, respectively. In Fig. 7, the equivalent optical depth $\tilde{\tau}(r)$ is depicted as a function of r/R_0 for different combinations of the r_{in} and r_h corresponding to different values of the black hole spin angular momentum (see Zhang, Cui and Chen 1997 for details). The slight turn over near the inner disk boundary is due to the existence of the black hole horizon, although no other general relativity effects are taken into account for the Compton scattering process near the black hole horizon.

In the multi-color disk blackbody model, the local disk radiation is assumed to be blackbody, i.e., its surface brightness follows the Planck distribution $B(T(r),\nu) = \frac{2h\nu^3}{c^2(e^{h\nu/kT(r)}-1)}$, and $T(r) = T_{in}(r/r_{in})^{-3/4}$. Therefore the average non-scattering probability for a photon with a frequency ν can be calculated as

$$\bar{P}(\nu) = \frac{\int_{r_{in}}^{\infty} 2\pi r B(r,\nu)\bar{P}(r)dr}{\int_{r_{in}}^{\infty} 2\pi r B(r,\nu)dr} \tag{10}$$

The equivalent optical depth for a photon with a frequency ν is thus

$$\tilde{\tau}(\nu) = -\ln\bar{P}(\nu) \tag{11}$$

If both R_0 and $n_{e,0}$ are known, then $P(\nu)$ and thus $\tau(\nu)$ can be calculated. It is easy to show that $\tilde{\tau}(r) \sim n_{e,0}a_e r_g \ln(R_0/r_{in})$, if $r \sim r_{in}$ and $R_0 \gg r_{in}$. It then follows that $\tilde{\tau}(\nu) \sim n_{e,0}a_e r_g \ln(R_0/r_{in})$, if $h\nu \sim kT_{in}$. This also implies that $n_{e,0}$ and R_0 are coupled together in $n_{e,0}a_e r_g \ln(R_0/r_{in})$. In Fig. 8, the equivalent optical depth $\tilde{\tau}(\nu)$ is depicted as a function of the emitted photon energy, for different combinations of $n_{e,0}$ and R_0, which are coupled together

by $n_{e,0}a_e r_g \ln(R_0/r_{in}) = constant$; the initial value of the constant is determined by taking $R_0 = 10^5$, $n_{e,0} = 10^{17}/cm^3$ (all radius are in units of the gravitational radius of the black hole, i.e., $r_g = GM/c^2$); $kT_{in} = 1.0$ keV. The left figure corresponding to the Schwarzschild geometry, i.e., $r_{in} = 6$ and $r_h = 2$; the right one is for a near-extremal Kerr black hole with $r_{in} = 2$ and $r_h = 1$.

Once $P(\nu)$ is known, we can derive the initial disk spectrum $F_i(\nu)$ from the observed disk spectrum $F_o(\nu)$ (the *diskbb* component in Eq. (2)):

$$F_i(\nu) = \frac{F_o(\nu)}{\cos i} e^{\tilde{\tau}(\nu)} \tag{12}$$

where i is the inclination angle of the accretion disk.

As we mentioned above, R_0 may be estimated by examining the phase-lag spectrum of its light curve. On the other hand, the value of $n_{e,0}$ may be calculated from the following radiative transfer equation:

$$\int F(compTT, \nu) d\nu = \frac{1}{\cos i} \int F_o(diskbb, \nu)(e^{\tilde{\tau}(\nu)} - 1) d\nu \tag{13}$$

where $F(compTT, \nu)$ and $F_o(diskbb, \nu)$ are the observed power-law and blackbody-like *photon* spectra, respectively.

Finally we can use the corrected accretion disk emission spectrum to estimate the inner accretion disk radius. First we can obtain the total blackbody-like flux:

$$F(BB) = \int h\nu F_o(diskbb, \nu) e^{\tilde{\tau}(\nu)} d\nu \tag{14}$$

Then we can apply the Eq. (3) in Zhang, Cui and Chen (1997) to estimate the inner accretion disk radius, i.e., the radius of the last stable orbit of the black hole.

It should be noted that the escaped spectrum also has a slightly different shape than the original spectrum, due to the frequency dependency of the equivalent optical depth $\tilde{\tau}(\nu)$. In Fig. 9, we show the escaped spectrum, i.e., the observed one, corresponding to different configurations of the corona, for a Schwarzschild black hole (*left figure*: $r_{in} = 6$ and $r_h = 2$) and a Kerr black hole (*right figure*: $r_{in} = 2$ and $r_h = 1$). The values of $n_{e,0}$ and R_0 are *not* allowed to change independently, i.e., are coupled together by $n_{e,0} \ln(R_0/r_{in}) = constant$ (the initial value of the constant is determined by taking $R_0 = 10^5$, $n_{e,0} = 3 \times 10^{17}/cm^3$); only values of R_0 are marked in the figures. The original disk spectrum without any scattering is also shown for comparison ($kT_{in} = 1.0$ keV). It is clear that the difference of the spectral shape from the original spectrum is in general very small, especially at energies $> kT_{in}$, unless when $R_0 \sim 10^2$. For the Kerr black hole, the escaped spectral shape is closer to the original one for the same corona configuration; however, the same spectral shape may be produced for both types of black holes, by taking different corona configurations.

Appendix B. The Color Correction

Even after the soft component is properly extracted from the observation data, proper color correction to the component is still required, since the emerged spectrum from the disk is actually not purely blackbody, due to electron scattering in the disk. In the optically thick disk the electron scattering is saturated (optical depth significantly greater than unity), thus the escaped spectrum may still be described as a multi-color blackbody model, in which the local spectrum is described by a diluted blackbody spectrum:

$$B'(h\nu, T'(r)) = \frac{1}{f_{col}^4} B(h\nu, f_{col}T(r)) \tag{15}$$

where B is the Planck function and f_{col} is the color correction factor Therefore the inferred disk radius is proportional to f_{col}^2. Previously the value of f_{col} has been estimated using theoretical calculations and assumed a constant in most cases. However, since the real value of the color correction depends on the property of the electron gas in the disk, in principle the color correction factor may not be a constant for a source in different spectral and luminosity states.

We may also model the soft component with the *compTT* model, from which we can obtain directly the temperature (T_0) of the seed photons. If the seed photon spectrum is *diskbb*, instead of blackbody assumed in the *compTT* model, the *real* inner disk temperature of the disk should be $kT_0 * 2.7$. Thus according to the definition of the color correction, $f_{col} = T_{in}/2.7kT_0$, in which T_{in} is obtained by fitting the same soft component with the *diskbb* model. The consistency of this approach may be examined by comparing T_{in} and T_e, which is the electron temperature inferred in the *compTT* model fitting; we should have $T_{in} \approx T_e$ if the observed soft component is indeed produced by saturated thermal Comptonization in the disk. In Fig. 10 we show one simulation for the ASCA GIS instrument, in which the input spectrum is generated from the *compTT* model (parameters shown in the figure), and the data are then fitted with both *compTT* and *diskbb* models. It is clear that the *diskbb* model also provides adequate fit to the data, and $T_{in} \approx T_e$

This offers a simple way for estimating the color factor from the observation data, thus avoiding many uncertainties in theoretical calculations and the assumption that the color correction factor is universally the same for all sources in all observations. There is, however, one restriction for applying this color correction method: the low energy response of the instrument must be good enough to allow kT_0 to be determined accurately. We have carried a series of simulations for evaluating capability of the existing instruments. We found that the ASCA instruments are the best suitable for this purpose, though the SAX instruments are comparable in performance. However, the RXTE instruments do not have the adequate low energy response for estimating the color correction factor this way.

We thus analyzed some ASCA archival data on GRO J1655-40 when the source was active. The results are summarized in figures 5-8. It can be seen that the corrected inner disk radius for all observations is consistent to a constant, despite the large spectral and flux variations between these observations over several years. This demonstrates that this technique in estimating the color correction factor is quite reasonable and that the inner accretion radius is indeed very

stable. We argue this as the most convincing evidence for the stability of the inner accretion disk boundary in a black hole X-ray binary.

REFERENCES

Belloni, T., Mendez, M., King, A. R., van der Klis, M., & van Paradijs, J. 1997, ApJ, 488, 109

Blandford, R. D., Znajek, R. L., 1977, MNRAS, 179, 433

Blandford, R. D., Begelman, M. C., 1999, MNRAS, 303L, 1

Campbell-Wilson, D., McIntyre, V., Hunstead, R., & Green, A. 1998, IAU Circ.7010

Casares, J., Dubus, G., Homer, L., 1999, IAU Circ.7113

Castro-Tirado, A.J., Duerbeck, H.W., Hook, I., Yan, L., 1998, IAU Circ.7013

Cui, W., Zhang, S.N., Chen, W., 1998, ApJ, 492L, 53

Cui, W., Zhang, S.N., Chen, W., Morgan, E.H., 1999a, ApJ, 512, L43 (Paper I)

Cui, W., Wen, L., Zhang, S.N., Wu, X.-B., 1999b, IAU Circ.7191

Ebisawa, K., Ogawa, M., Aoki, T., Dotani, T., Takizawa, M., Tanaka, Y., Yoshida, K., Miyamoto, S., Iga, S., Hayashida, K., Kitamoto, S., & Terada, K. 1994, PASJ, 46, 375

Finger, M.H., Dieters, S.W., Wilson, R.B., 1998, IAU Circ.7010

Hameury, J.-M., Lasota, J.-P., McClintock, J. E. & Narayan, R. 1997, ApJ, 489, 234

Harmon, B.A., Finger, M.H., McCollough, M.L., Zhang, S.N., Paciesas, W.S., Wilson, C.A., 1999, IAU Circ.7098

Hjellming, R. M. & Rupen, M. P. 1995, Nature, 375, 464

Homan, J., Wijnands, R., van der Klis, M., 1999, IAU Circ.7121

Hynes, R. I., Haswell, C. A., Shrader, C. R., Chen, W., Horne, K, Harlaftis, E. T., O'Brien, K., Hellier, C. & Fender, R. P. 1998, MNRAS, 300, 64

Hua, X.-M., Kazanas, D. & Cui, W., 1999, ApJ, 512, 793

Jain, R., Bailyn, C. D., McClintock, J.E., Sobczak, G.J., Remillard, R. A., Orosz, J. A., 1999a, IAU Circ.7114

Jain, R., Bailyn, C. D., Greene, J., McClintock, J.E., Remillard, R. A., 1999b, IAU Circ.7187

Jain, R., Bailyn, C. D., Orosz, J. A., Remillard R. A., & McClintock, J. E. 1999c, ApJ, 517, L131

Levine, A. M., Bradt, H., Cui, W., Jernigan, J. G., Morgan, E. H., Remillard, R., Shirey, R. E., & Smith, D. A. 1996, ApJ, 469, 33

McClintock, J.E., Sobczak, G.J., Remillard, R. A., Morgan, E.H., Levine, A. M., 1998, IAU Circ.7025

Makishima, K., Maejima, Y., Mitsuda, K., Bradt, H. V., Remillard, R. A., Tuohy, I. R., Hoshi, R., & Nakagawa, M. 1986, ApJ, 308, 635

Marshall, F.E., Smith, D.A., DOtani, T., Ueda, Y., 1998, IAU Circ.7013

Merloni, A., Fabian, A.C., Ross, R.R. 1999, MNRAS, 313, 193.

Mirabel, I. F. & Rodriguez, L. F. 1998, Nature, 392, 673

Mitsuda, K., *et al.*, 1984, PASJ, 36, 741

Morrison, R. & McCammon, D. 1983, ApJ, 270, 119

Narayan, R. 1995, ApJ, 462, 136.

Narayan, R. & Yi, I. 1995, ApJ, 444, 231.

Orosz, J. A., Bailyn, C. D. 1997a, ApJ, 474.

Orosz, J., Remillard, R. A., Bailyn, C. D., McClintock, J. E. 1997b, ApJ, 478, L83

Orosz, J., Bailyn, C., & Jain, R. 1998, IAU Circ.7009

Remillard, R. A., McClintock, J. E., Sobczak, G. J., Bailyn, C. D., Orosz, J. A., Morgan, E. H., & Levine, A. M. 1999a, ApJ, 517, L127

Remillard, R. A., Morgan, E.H., McClintock, J.E., Sobczak, G.J., 1998, IAU Circ.7019

Remillard, R. A., Morgan, E.H., McClintock, J.E., Sobczak, G.J., Bailyn, C. D., Jain, R., 1999b, IAU Circ.7123

Sánchez-Fernández, C., *et al.*, 1999, A&A, in press (astro-ph/9906434)

Shahbaz, T., van der Hooft, F., Casares, J., (IAC), Charles, P.A., van Paradijs J. 1999, MNRAS, 306, 89-94.

Shakura, N. I. & Sunyaev, R. A. 1973, A&A, 24, 337

Shimura, T. & Takahara, F. 1995, ApJ, 445, 780

Smith, D. A. & RXTE/ASM teams 1998, IAU Circ.7008

Sobczak, G. J., McClintock, J. E., Remillard, R. A., Bailyn, C. D., Orosz, J. A., 1999a, ApJ, 520, 776.

Sobczak, G. J., McClintock, J. E., Remillard, R. A., Levine, A. M., Morgan, E. H., Bailyn, C. D., & Orosz, J. A., 1999b, ApJ, 517, L121

Sunyaev, R.A., & Titarchuk, L.G., 1980, A&A, 86, 121

Tingay, S. J., Jauncey, D. L., Preston, R. A., Reynolds, J. E., Meier, D. L., Murphy, D. W., Tzioumis, A. K., McKay, D. J., Kesteven, M. J., Lovell, J. E. J., Campbell-Wilson, D., Ellingsen, S. P., Gough, R., Hunstead, R. W., Jones, D. L., McCulloch, P. M., Migenes, V., Quick, J., Sinclair, M. W., Smits, D., 1995, Nature, 374, 141

Titarchuk, L. 1994, ApJ, 434, 313.

Titarchuk, L.G. & Lyubarskij, Yu., 1995, ApJ, 450, 876

Wilson, C. A., Harmon, B. A., Paciesas, W. S., & McCollough, M. L. 1998, IAU Circ.7010

Zhang, S. N., *et al.*, 1994, IAU Circ. 6046.

Zhang, S. N., Ebisawa, K., Sunyaev, R., Ueda, Y., Harmon, B. A., Sazonov, S., Fishman, G. J., Inoue, H., Paciesas, W. S., & Takahashi, T. 1997a, ApJ, 479, 381

Zhang, S. N., Cui, W., & Chen, W. 1997b, ApJ, 482, L155

Zhang, S. N., Wu, X.-B., Sun, X.J., Yao, Y. S., Cui, W., Chen, W. 1999, in preparation

Zhang, S. N., Cui, W., Chen, W., Yao, Y.S., Zhang, X.L., Sun, X.J., Wu, X.-B., Xu, H.G., 2000, Science, 287, 1239

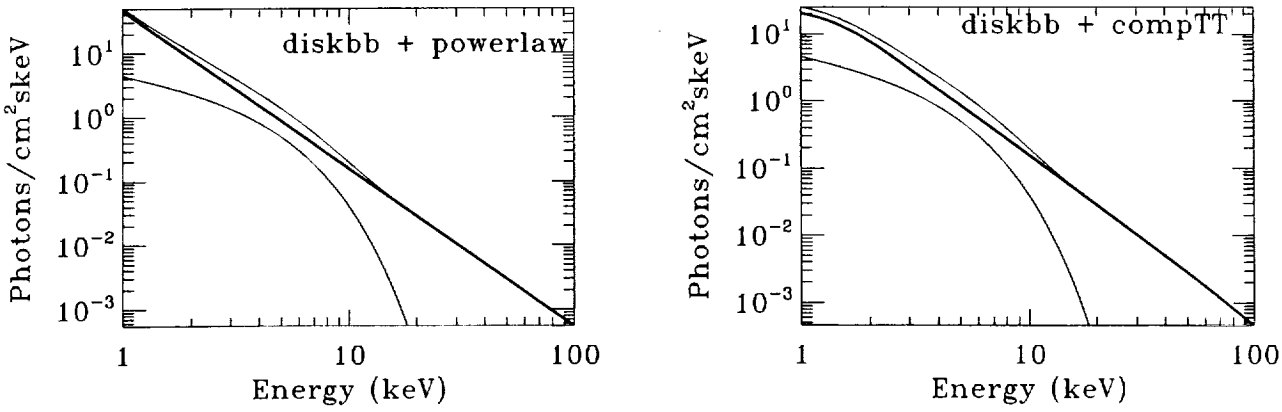

Fig. 3.— Comparison between *power-law* and *compTT* model. Notice the cut-off at low energy end of the *compTT* model and the slightly underestimation of the *diskbb* normalization.

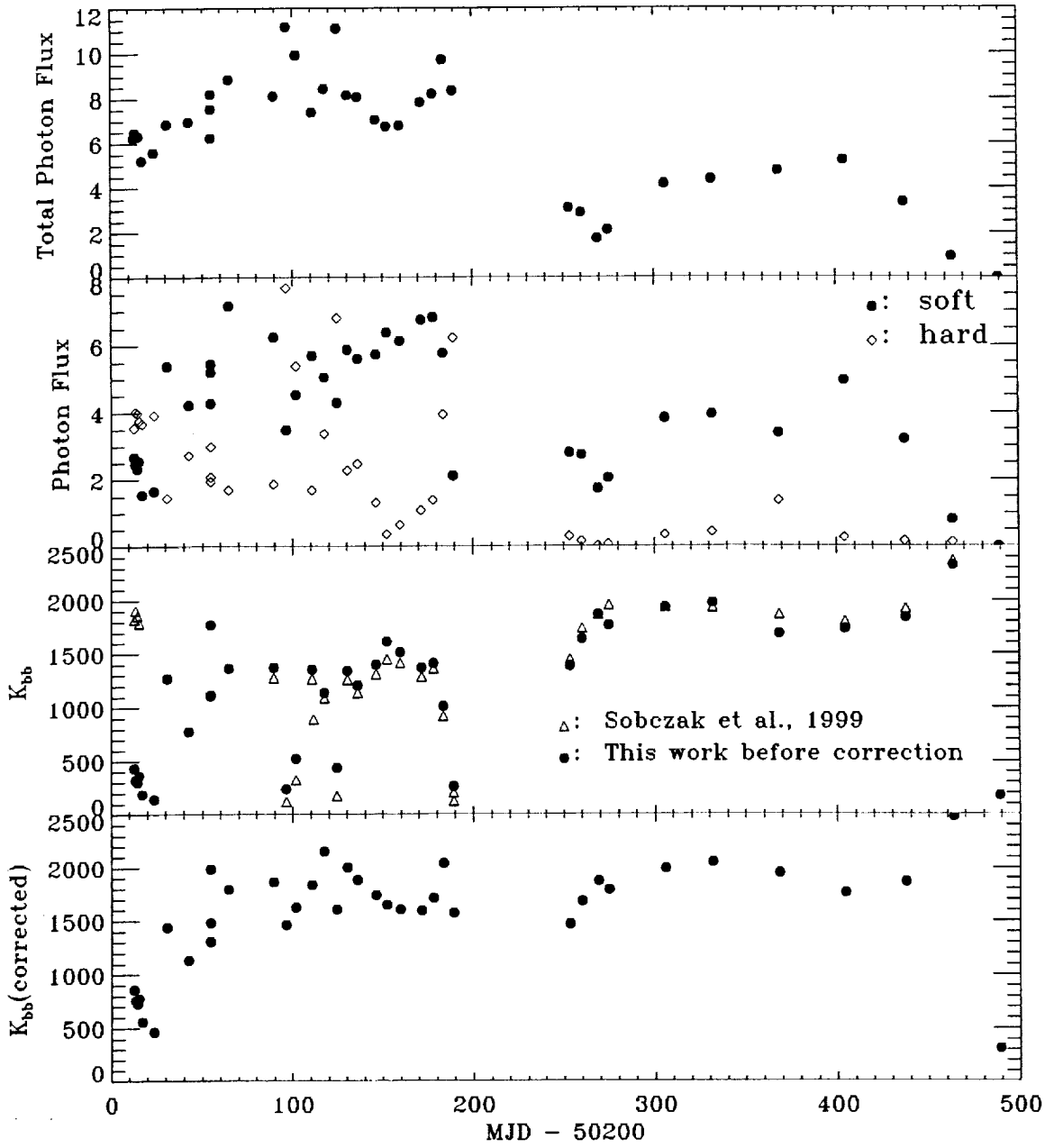

Fig. 4.— The main results of our work. It can be seen that the observed soft component normalization varies dramatically in the very-high/variable state. Also there is a significant anti-correlation between the hard photon flux and the soft component normalization, which indicates that they must be of the same origin and provides evidence for the necessity of Comptonization radiative correction. The bottom panel shows the soft component normalization after the correction, which is much more stable. Photon flux in this figure is in 2.5 - 20 keV.

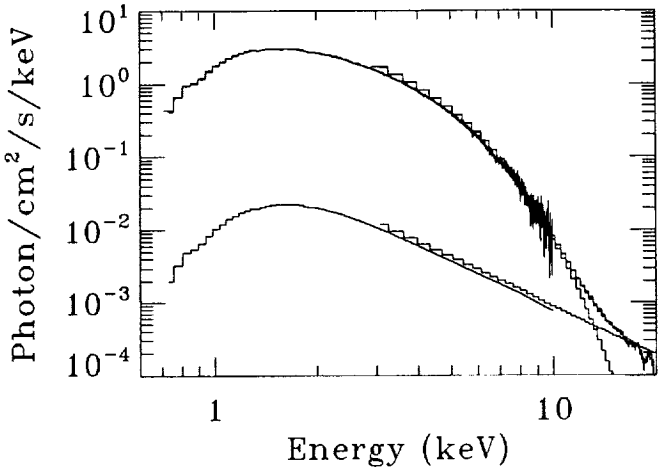

Fig. 5.— Joint fitting of ASCA and XTE data from the observation taken in 970226. The ASCA/GIS2 data in 0.7 - 10 keV and XTE/PCA data in 2.5 - 20 keV are used. There exists a significant difference between the ASCA and XTE normalizations (Refer to Table 2).

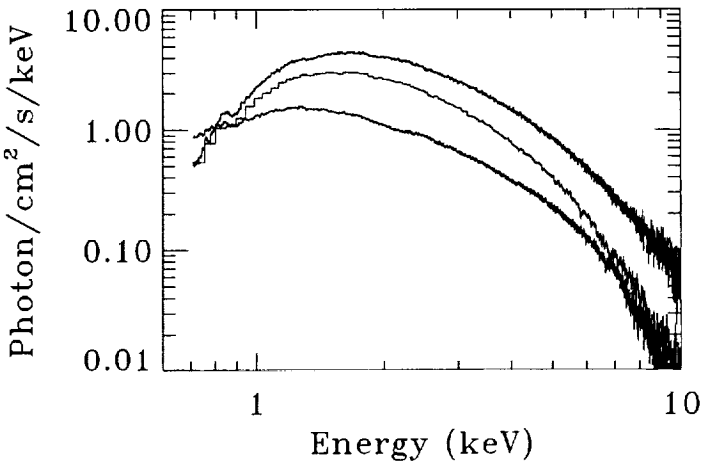

Fig. 6.— Three ASCA observations taken in 970226, 950815 and 940927 (from top to bottom), when the source is in soft state and the hard component is negligible, therefore the Compton radiative correction is not necessary. It can be seen that the spectral shape and normalization varies significantly. However, the derived color correction factor is not constant, the inferred since the but the inner disk radius (after color correction) remains rather stable (Refer to Table 5).

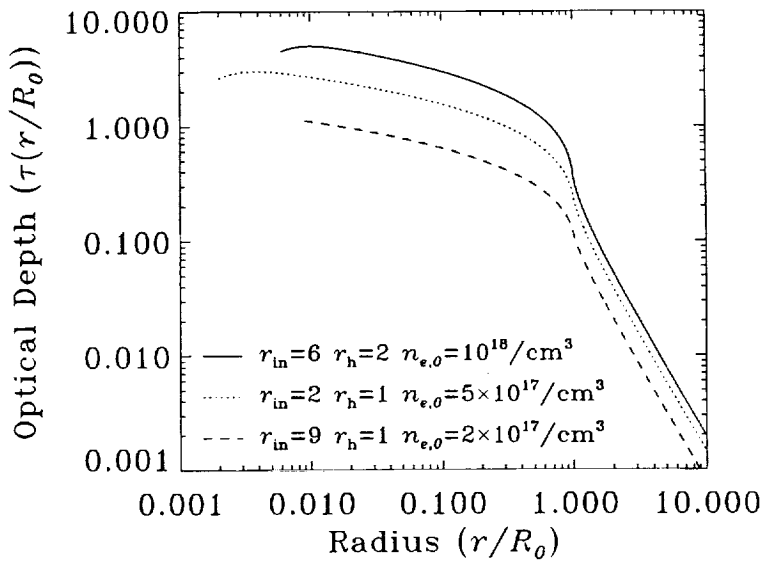

Fig. 7.— The equivalent optical depth $\tilde{\tau}(r)$ is depicted as a function of r/R_0 for different combinations of the r_{in} and r_h corresponding to different values of the black hole spin angular momentum (see Zhang, Cui and Chen 1997 for details). The slight turn over near the inner disk boundary is due to the existence of the black hole horizon, although no other general relativity effects are taken into account for the Compton scattering process near the black hole horizon.

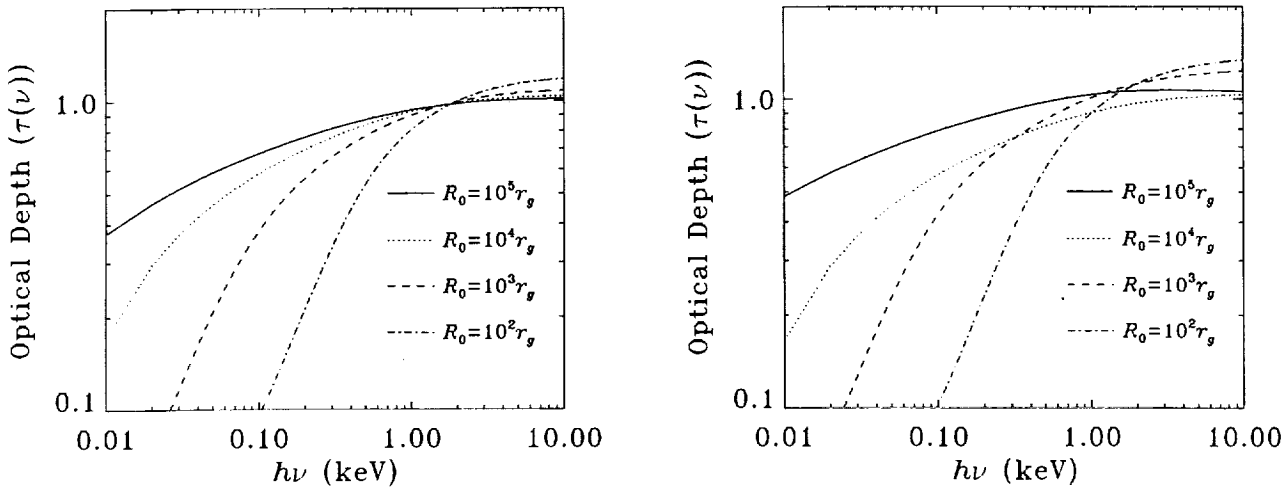

Fig. 8.— The equivalent optical depth $\tilde{\tau}(\nu)$ depicted as a function of the emitted photon energy, for different combinations of $n_{e,0}$ and R_0, which are coupled together by $n_{e,0} a_e r_g \ln(R_0/r_{in}) = constant$; the initial value of the constant is determined by taking $R_0 = 10^5$, $n_{e,0} = 10^{17}/cm^3$ (all radius are in units of the gravitational radius of the black hole, i.e., $r_g = GM/c^2$); $kT_{in} = 1.0$ keV. The *left* figure corresponding to the Schwarzschild geometry, i.e., $r_{in} = 6$ and $r_h = 2$; the *right* one is for a near-extremal Kerr black hole with $r_{in} = 2$ and $r_h = 1$.

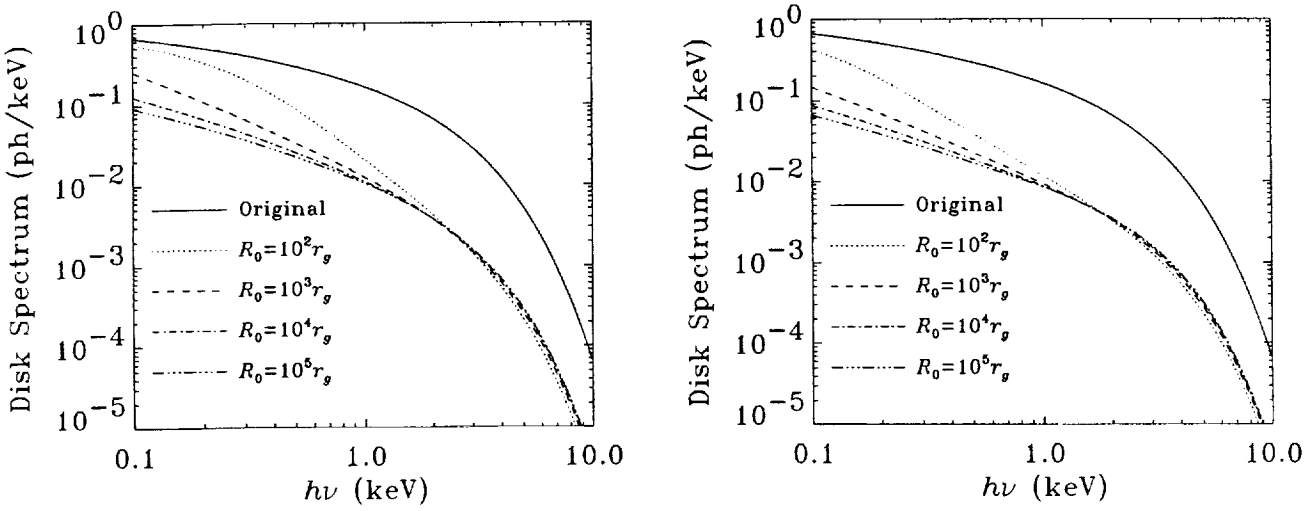

Fig. 9.— The escaped spectrum, i.e., corresponding to different configurations of the corona, for a Schwarzschild black hole (*left figure*: $r_{in} = 6$ and $r_h = 2$) and a Kerr black hole (*right figure*: $r_{in} = 2$ and $r_h = 1$). The values of $n_{e,0}$ and R_0 are *not* allowed to change independently, i.e., are coupled together by $n_{e,0} \ln(R_0/r_{in}) = constant$ (the initial value of the constant is determined by taking $R_0 = 10^5$, $n_{e,0} = 3 \times 10^{17}/cm^3$); only values of R_0 are marked in the figures. The original disk spectrum without any scattering is also shown for comparison ($kT_{in} = 1.0$ keV). It is clear that the difference of the spectral shape from the original spectrum is in general very small, especially at energies $> kT_{in}$, unless when $R_0 \sim 10^2$.

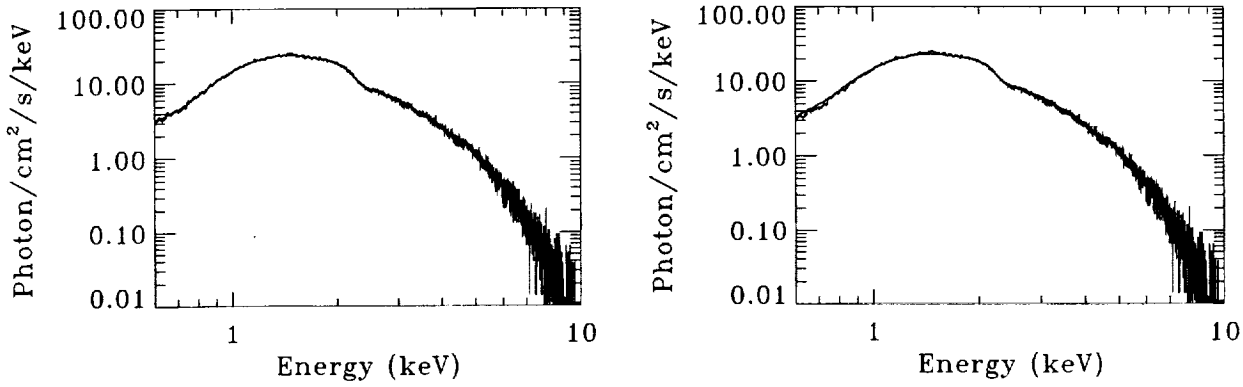

Fig. 10.— Simulation for fitting thermal Compton spectrum with *diskbb* model in XSPEC. The simulated data are produced with the *compTT* model. The data are then fit with both *compTT* (left) and *diskbb* (right) models, both producing adequate fitting. Data parameters: $T_0 = 0.30, T_e = 1.0$keV$, \tau = 10$; Fitting parameters with *compTT* model: $T_0 = 0.29, T_e = 0.94$keV$, \tau = 11.0$; Fitting parameters with *diskbb* model: $T_{in} = 0.96$keV.